This is an *Accepted Manuscript*, which has been through the Royal Society of Chemistry peer review process and has been accepted for publication.

Accepted Manuscripts are published online shortly after acceptance, before technical editing, formatting and proof reading. Using this free service, authors can make their results available to the community, in citable form, before we publish the edited article. We will replace this *Accepted Manuscript* with the edited and formatted *Advance Article* as soon as it is available.

You can find more information about *Accepted Manuscripts* in the **Information for Authors**.

Please note that technical editing may introduce minor changes to the text and/or graphics, which may alter content. The journal's standard **Terms & Conditions** and the **Ethical guidelines** still apply. In no event shall the Royal Society of Chemistry be held responsible for any errors or omissions in this *Accepted Manuscript* or any consequences arising from the use of any information it contains.

Dalton Transactions

ARTICLE

Uranyl-Oxo Coordination Directed by Non-Covalent Interactions

Andrew J. Lewis, Haolin Yin, Patrick J. Carroll, Eric J. Schelter

Directed coordination of weakly Lewis acidic K+ ions to weakly Lewis basic uranyl oxo ligands is accomplished through non-covalent cation-π and cation-F interactions for the first time. Comparison of a family of structurally related diarylamide ligands highlights the role that the cation-π and cation-F interactions play in guiding coordination. Cation binding to uranyl and U=O bond activation is demonstrated in the solid state and in solution, providing the shortest reported crystallographic uranyl-oxo-potassium distance. UV-Vis, TD-DFT calculations, and electrochemical measurements show that cation coordination directly impacts the electronics at the uranium(VI) cation.

Introduction

The uranyl ion (UO_2^{2+}) is the most prevalent form of uranium in Nature, due to the thermodynamic stability of the linear *trans*-dioxo arrangement of oxygen atoms at the uranium(VI) cation.[1] It is of interest to develop new methods for activating U=O bonds in the context of the treatment of uranium-bearing waste, to develop bioremediation approaches wherein uranyl is converted to low solubility oxides such as uraninite, and to expand the fundamental chemistry of the moiety. [2, 3] Various strategies have been employed to activate the inert uranium-oxo bonds of uranyl.[3] For example, photo-excitation of electrons localized in U=O bonding orbitals to non-bonding U(5f) orbitals facilitates reactivity of the U=O bond.[4] In terms of design, strong σ-donating ligands polarize U=O bonds as a consequence of *cis*-destabilization, a feature of the inverse *trans* influence present in high-valent uranium complexes.[1, 5-9] Such polarization of the U=O bonds increases the Lewis basicity of the oxo ligands, causing them to be more prone to Lewis acid coordination.[10] In such scenarios, Lewis acid coordination reduces the charge donation from the oxo ligand to the uranium center, which weakens the U=O bond and facilitates reduction at uranium. Reduction to uranium(V) weakens the U=O bonds, making further reactivity accessible.[11-13] Lewis acid coordination has therefore been recognized as a key component of U=O bond activation in several reported systems.

In the absence of strongly σ-donating ligands, the uranyl oxo ligands tend to be only weakly Lewis basic, requiring strong Lewis acids such as $B(C_6F_5)_3$ to achieve coordination.[10] The formation of strong B–O and Si–O bonds can also provide a substantial enthalpic driving force for U=O bond activation.[13-17] Directing Lewis acid coordination to uranyl has been accomplished through the use of flexible, Pacman-type ligands,

a highly successful strategy developed by Arnold and co-workers (Fig. 1, left).[11, 12, 18-25] The simplest Lewis acid, H+, was directed towards interaction with UO_2^{2+} in the stereognostic coordination chemistry developed by Raymond and co-workers (Fig. 1, right).[26] Weaker Lewis acids such as alkali metal cations are also known to bind to uranyl oxo-groups in a variety of cases, employing much simpler ligand designs.[27-34]
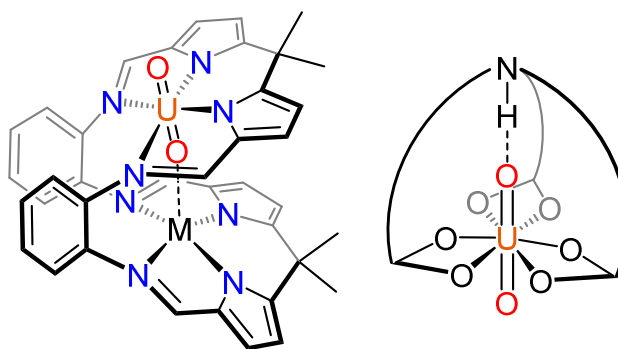

Fig. 1 Lewis acid coordination to uranyl directed by macrocyclic Schiff-base (left) and tris[2-(2-carboxyphenoxy)alkyl]ammonium ligands (right).[25, 26]

Toward our goal of manipulating the coordination environments around f-block cations through collective non-covalent interactions in secondary coordination spheres,[35-39] we sought to facilitate Lewis acid binding at only weakly Lewis basic uranyl oxo ligands through the use of supramolecular design principles. In our recent work exploring the coordination chemistry of electron-poor diarylamide ligands,[35, 40, 41] we determined that these ligands provided a suitable coordination environment around uranium to create discrete, monomeric complexes. In this contribution, we demonstrate that a coordination pocket that promotes potassium cation binding can

be organized at uranyl-oxo ligands using an ensemble of non-covalent interactions.

Considering the coordination chemistry of fluorinated diarlyamides with the uranyl cation, we reasoned that these diarylamide ligands, including $NPh^F_2{}^-$ (Ph^F = pentafluorophenyl), NPh^FPh^-, NPh^Fpy^- (py = 2-pyridyl), and NAr^FPh^- (Ar^F = 3,5-bis(trifluoromethyl)phenyl), would create a pocket lined with aryl-fragments around each of the U=O bonds, which could serve as a scaffold to direct cation binding. In this contribution, we focus on directing the coordination of relatively weakly Lewis acidic K^+ ions to uranyl through self-assembly directed by cation-π and cation-fluorine interactions. The K^+ ion serves as a proof of principle of this approach, as it has only a small inherent tendency to interact with uranyl oxo ligands. For example, among complexes of the formula $[M(crown)]_2[UO_2X_4]^{2-}$ (M(crown) = Li(12-crown-4)$^+$, Na(15-crown-5)$^+$, K(18-crown-6)$^+$, X = Cl$^-$, Br$^-$), M–O=U coordination preference follows the trend Li$^+$ > Na$^+$ > K$^+$.[27] We also demonstrate that K^+ coordination directed by the fluorinated diarylamide ligands provides discernable modulation of the O=U=O electronic structure that persists in solution.

Results and Discussion
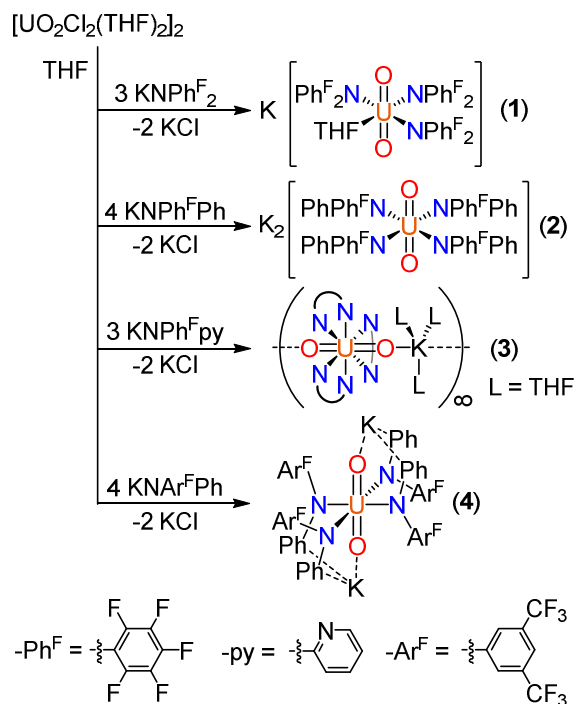
Scheme 1 Synthesis of compounds **1**-**4**.

We first attempted to prepare a uranyl complex of $NPh^F_2{}^-$, a ligand that is prone to forming F→M$^+$ interactions.[35, 39, 42] Reaction of 3 or more equiv $KNPh^F_2$ with $[UO_2Cl_2(THF)_2]_2$ led to formation of a 3:1 ligand:uranyl complex as judged by ^1H NMR (Scheme 1). Crystallization of this orange product from a

THF solution layered with hexanes allowed for structural determination as $[K(THF)_5][UO_2(NPh^F_2)_3(THF)]$ (**1**) (Fig. 2).
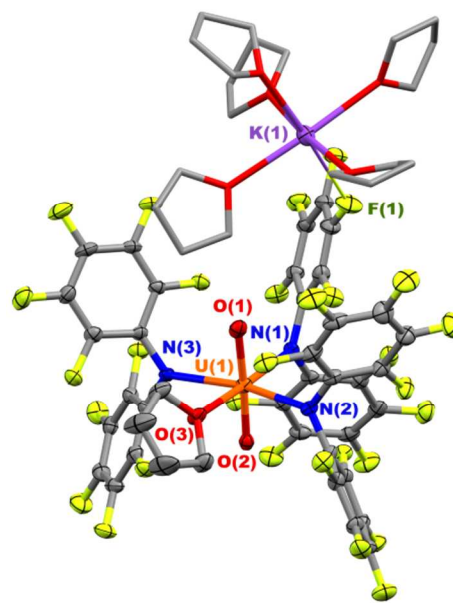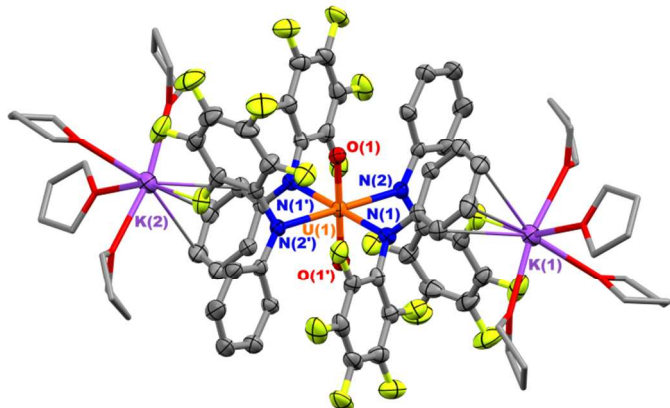
Fig. 2 Thermal ellipsoid plot of **1** at 30% probability. Hydrogen atoms are omitted and THF-K$^+$ solvation is shown as capped sticks for clarity. Selected bond distances (Å) and angles (deg): U(1)–O(1) 1.770(6), U(1)–O(2) 1.772(5), U(1)–O(3) 2.446(4), U(1)–N(1) 2.378(5), U(1)–N(2) 2.386(6), U(1)–N(3) 2.390(6), O(1)–U(1)–O(2) 177.0(2).

The structure of **1** exhibited close contact of the potassium ion with a single fluorine atom of one of the –Ph^F groups at 2.995(6) Å, but the orientation of the C–F bond directed the K$^+$ ion away from the uranyl center, preventing it from direct interaction with the uranyl oxygen atoms. The U=O distances of **1**, 1.770(6) and 1.772(5) Å, were consistent with reported, unactivated uranyl complexes.[43] The room temperature ^{19}F NMR for **1** showed three resonances in a 2:2:1 ratio, indicative of chemical equivalency of the three amide ligands, ruling out strong association of the K$^+$ ion in solution. Attempts to coordinate a fourth equivalent of amide to **1** to alter the geometry led to no reaction, likely due to the electron deficient nature of the ligand as well as steric hindrance. We reasoned that the slightly more electron rich ligand NPh^FPh^- could allow for coordination of a fourth ligand, and therefore incorporation of a second potassium cation.

The reaction of 8 equiv $KNPh^FPh$ with $[UO_2Cl_2(THF)_2]_2$ produced a red solid (Scheme 1), which was obtained as a crystalline product by layering a THF solution with hexanes. The X-ray crystal structure of this product revealed the formula to be $[K(THF)_5]_2[UO_2(NPh^FPh)_4]$ (**2**) (Fig. 3). As in **1**, the structure of **2** demonstrated close contacts of the potassium ions with fluorine atoms on the periphery of the –Ph^F rings at 2.773(4) Å. Cation-π interactions between the K$^+$ ion and two phenyl groups were also noted in the structure of **2**, at a close contact distance of ~3.12 Å. However, these interactions collectively directed the K$^+$ ions away from the U=O moiety. We reasoned that re-orienting these –Ph^F groups by tethering the other aryl substituent to the metal center could effectively

increase the pocket size and thus more favourably align the fluorine atoms to direct K$^+$ ion binding to the uranyl oxo ligands.

Fig. 3 Thermal ellipsoid plot of **2** at 30% probability. Hydrogen atoms are omitted and THF-K$^+$ solvation is shown as capped sticks for clarity. Selected bond distances (Å) and angles (deg): U(1)–O(1) 1.765(3), U(1)–N(1) 2.442(4), U(1)–N(2) 2.424(4), O(1)–U(1)–O(2) 180.0(2).

Addition of 6 equiv KNPh^{F}py to [UO$_2$Cl$_2$(THF)$_2$]$_2$ (Scheme 1) produced a red product that was identified by X-ray structural analysis as [K(THF)$_3$][UO$_2$(NPh^{F}py)$_3$] (**3**) (Fig 4). The crystal structure of **3** revealed an 8-coordinate uranium center in which each of the amide ligands bind through both the 2-pyridyl nitrogen as well as the amide nitrogen. The orientation of the –Ph^F groups promoted π-stacking, at a centroid-to-centroid distance of 3.37 Å between two of the –Ph^F rings. This binding motif oriented the C–F bonds of the –Ph^F groups such that the *ortho*-fluorine from each –Ph^F group directed K$^+$ ion coordination to the U=O moieties, at an average K–O distance of 2.714(8). Due to the poor resolution of the X-ray structure, the U=O bond distances, at 1.777(8), are indistinguishable from those of **1** or **2** within statistical error. Despite crystallization from THF, the K$^+$ ions were only solvated by three THF molecules, with additional coordination to two fluorine atoms and two uranyl oxo ligands in a 1D chain coordination polymer. This O=U^{VI}=O−K polymeric chain structure is reminiscent of the ionic coordination polymer complex [U^{V}O$_2$(py)$_5$][KI$_2$(py)$_2$]$_\infty$,[44, 45] in which K$^+$ ions also bridge between multiple UO$_2^+$ ions. However, in the uranium(V) form, this interaction is expected to be more favourable due to the weakening of the U=O bonds as well as the build-up of negative charge on the oxo groups. The room temperature ^{1}H and ^{19}F NMR spectra of **3** reveal chemical equivalence of the amide ligands, similarly suggesting that the K$^+$ is not associated with the anion in solution.
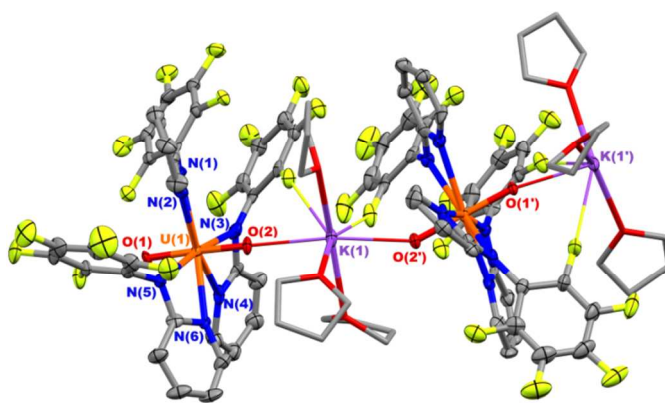
Fig. 4 Thermal ellipsoid plot of **3** at 30% probability. Hydrogen atoms are omitted and THF-K$^+$ solvation is shown as capped sticks for clarity. Selected bond distances (Å) and angles (deg): U(1)–O(1) 1.769(7), U(1)–O(2) 1.775(7), U(1′)–O(1′) 1.779(7), U(1′)–O(2′) 1.783(7), U(1)–N(1) 2.602(9), U(1)–N(2) 2.556(10), U(1)–N(3) 2.532(11), U(1)–N(4) 2.507(9), U(1)–N(5) 2.536(11), U(1)–N(6) 2.490(9), U(1′)–N(1′) 2.522(11), U(1′)–N(2′) 2.588(10), U(1′)–N(3′) 2.457(10), U(1′)–N(4′) 2.565(10), U(1′)–N(5′) 2.575(10), U(1′)–N(6′) 2.538(10), K(1)-O(1) 2.738(7), K(1)–O(2) 2.707(7), K(1′)-O(1′) 2.716(7), K(1′)–O(2′) 2.693(8), O(1)–U(1)–O(2) 178.0(4), O(1′)–U(1′)–O(2′) 178.4(4).

Expanding on the structural insight provided by complexes **1**–**3**, we sought to determine the impact of cation-π interactions in the absence of the perfluorophenyl group. Reaction of 8 equiv KNAr^{F}Ph with [UO$_2$Cl$_2$(THF)$_2$]$_2$ in THF led to an immediate color change to dark red (Scheme 1). Removal of solvent or addition of non-coordinating solvent such as hexanes led to a color change to dark green.[46] Extraction and recrystallization of the dark green product from toluene allowed for the isolation of [K(toluene)]$_2$[UO$_2$(NAr^{F}Ph)$_4$] (**4-tol**) in 71% yield. X-ray structural analysis of **4-tol** (Fig. 5) revealed close association of both potassium ions with the uranyl oxo ligands in the solid state at average K–O distances of 2.602(3). This K–O distance represents the shortest known contact between a K$^+$ ion and uranyl, including pentavalent uranyl complexes.[44, 45, 47]

The orientation of the aryl substituents around the U=O bond create a pocket that facilitates favorable cation-π binding, directing the K$^+$ ion to coordinate to the uranyl oxo ligands. Furthermore, it has been previously suggested that the encapsulation of the uranyl moiety in a hydrophobic pocket strengthens the equatorial metal-ligand bonding.[48] No short distances between the K$^+$ ions and the CF$_3$ groups were identified in the structure of **4-tol**. The ^{1}H NMR spectrum of **4-tol** displayed a minimal number of resonances and the ^{19}F NMR spectrum showed only one resonance, supporting a symmetric ligand arrangement consistent with the X-ray structure. Attempts to desolvate **4-tol** through application of dynamic vacuum or addition of non-coordinating solvent such as hexanes had no effect, indicating resilience of the potassium cations towards desolvation.
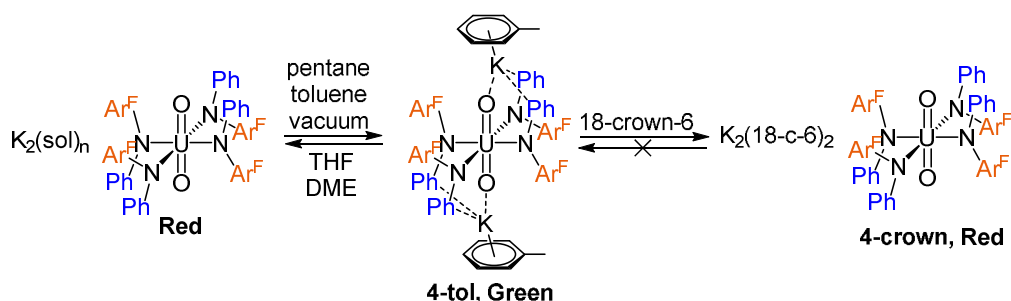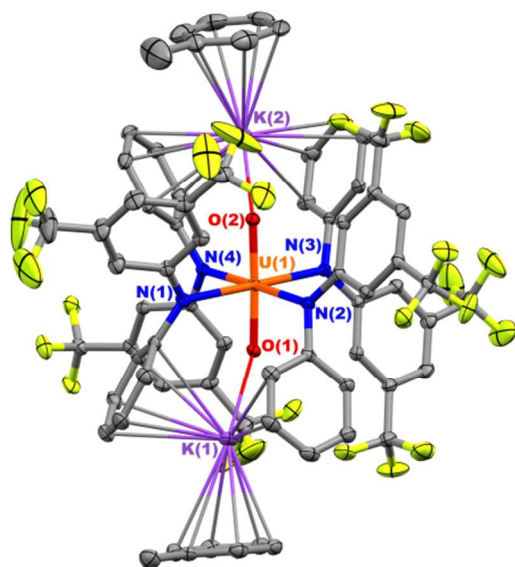
Scheme 2 Solvation dynamics of **4-tol** and **4-crown**.

Fig. 5 Thermal ellipsoid plot of **4-tol** at 30% probability. Hydrogen atoms omitted for clarity. Selected bond distances (Å) and angles (deg): U(1)–O(1) 1.802(2), U(1)–O(2) 1.806(2), U(1)–N(1) 2.402(3), U(1)–N(2) 2.375(3), U(1)–N(3) 2.396(3), U(1)–N(4) 2.398(3), K(1)–O(1) 2.589(2), K(2)–O(2) 2.615(3), O(1)–U(1)–O(2) 177.79(10).

Dissolution of **4-tol** in a coordinating solvent such as THF reversibly restored the dark red color (Scheme 2). Addition of 2 equiv 18-crown-6 to a toluene solution of **4-tol** led to immediate precipitation of a red solid. Recrystallization from DME layered with hexanes produced crystals suitable for X-ray diffraction, which revealed the structure to be [K(18-crown-6)(DME)]$_2$[UO$_2$(NAr^{F}Ph)$_4$] (**4-crown**) (DME = 1,2-dimethyoxyethane) (Fig. 6). With the exception of the removal of the K$^+$ ion from direct coordination to uranyl in **4-crown**, the overall structural arrangement of the different aryl functionalities is essentially the same as that of **4-tol**. Additionally, the ^{1}H NMR spectrum of **4-crown** indicated a similar symmetric ligand environment as in **4-tol**, and again the ^{19}F NMR displayed a single resonance.
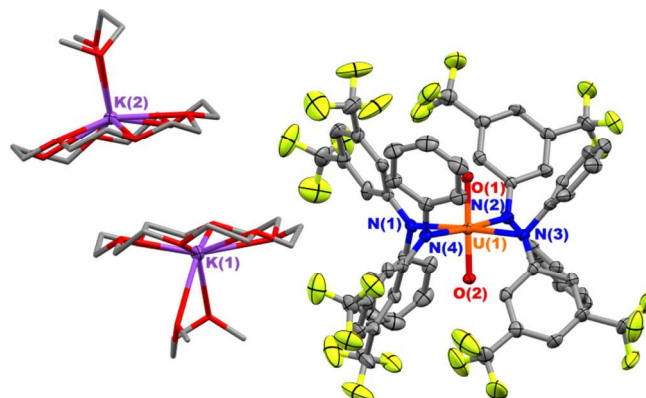

Fig. 6 Thermal ellipsoid plot of **4-crown** at 30% probability. Hydrogen atoms are omitted for clarity. Selected bond distances (Å) and angles (deg): U(1)–O(1) 1.789(4), U(1)–O(1) 1.792(4), U(1)–N(1) 2.420(5), U(1)–N(2) 2.453(5), U(1)–N(3) 2.442(5), U(1)–N(4) 2.434(5), O(1)–U(1)–O(2) 178.94(19).

Determining the extent of activation of the U=O bonds of uranyl from the bond metrics is limited by the small variation in these bond lengths. Typical U^{VI}=O bond lengths range from 1.70 to 1.85 Å depending on the degree of activation, though in practice most uranyl complexes exhibit bond lengths of ~1.77 Å within experimental error.[43] A slight lengthening of the U=O bonds in **4-tol** relative to those of **4-crown** is consistently observed, but the different bond lengths are too close to reliably differentiate (Table 1). However, within the conserved primary coordination environment, there is a statistically significant decrease in the U–N bond lengths upon K$^+$ ion coordination to uranyl (Table 1). These metrics imply that K$^+$–O coordination weakens the U=O bonds, which strengthens the equatorial U–N bonds through the inverse *trans* influence.[1, 5]

These U–N bond lengths are significantly longer than those of other structurally characterized uranyl complexes bound solely to amide ligands, including [Na(THF)$_2$][UO$_2$(N(SiMe$_3$)$_2$)$_3$] at 2.310(5),[31] and [Li(DME)$_2$Cl][Li(DME)][UO$_2$(NC$_5$H$_{10}$)$_2$(μ-NC$_5$H$_{10}$)]$_2$ at 2.249(7),[32] due to the electron-poor nature of the NAr^{F}Ph$^-$ ligand as well as the dianionic charge at uranium. In contrast, the U–N bonds in U(IV) complexes bearing the N(SiMe$_3$)$_2^-$ ligand are slightly longer than those containing the NAr^{F}Ph$^-$ ligand.[35, 49]

Table 1 Comparison of bonding metrics in **1-4**.

	U–O$_{av}$	U–N$_{av}$	K–O$_{av}$
1	1.771(8)	2.385(7)	–
2	1.765(4)	2.433(5)	–
3	1.777(8)	2.537(11)	2.714(8)
4-tol (exp.)	1.804(3)	2.393(2)	2.602(3)
4-tol (calc.)	1.807	2.449	2.589
4-crown (exp.)	1.791(6)	2.437(6)	–
4-crown (calc.)	1.783	2.489	–

DFT optimized geometries of the gas phase structures of **4-tol** and **4-crown** were obtained to support the observable differences in bond metrics (Table 1). As noted in the X-ray crystal structures, upon K$^+$ coordination a slight lengthening of the U=O bonds was noted, as well as a more significant shortening of the equatorial U–N bonds. Close agreement with the experimental K–O distances was obtained in the model of **4-tol**, though some preference for K$^+$–F interactions over K$^+$–Ph interactions was noted over the course of the optimization, leading to minor differences in the secondary structure, where one K$^+$ ion was coordinated to a single arene and two fluorine atoms.

Identification of the v_1 symmetric U=O stretching modes obtained from DFT frequency calculations established a shift from 854 cm^{-1} in **4-crown** to 807 cm^{-1} in **4-tol** (Fig. S6), indicative of weakening of the U=O bonds. For comparison, upon coordination of B(C$_6$F$_5$)$_3$ to UO$_2$(NCN)$_2$(THF) (NCN = [(SiMe$_3$N)$_2$CPh]$^-$), the v_1 mode shifts from 803 cm^{-1} to 780 cm^{-1}.[10] We were unable to locate the v_3 asymmetric U=O stretching mode by IR spectroscopy due to overlap with ligand-based vibrations (Fig. S1). Mayer bond order (MBO) analysis showed that K$^+$ coordination leads to a decrease in the average U=O MBO from 1.974 to 1.804 and an increase in the average U–N MBO from 0.462 to 0.525. Additionally, the natural charge localized on the oxygen atoms increased from –0.584 to –0.673 with K$^+$ coordination, signifying greater polarization of the U=O bonds. These metrics all support modulation (weakening) of the U=O bonds upon K$^+$ coordination.

Complexes **4-crown** (red) and **4-tol** (green) exhibited a dramatic difference in color, prompting us to collect electronic absorption spectra of these compounds. To rule out solvatochromism,[50] the absorption spectra of both compounds were collected in CH$_2$Cl$_2$, in which each compound retained its characteristic color. The intense bands of energies ≥ 3.5 eV were assigned to amide-ligand based π-π* and/or π*-π* electronic transitions (Fig. 7). The lower energy absorption bands, of energies ≤ 3.5 eV were assigned to LMCT transitions between the amide ligands and uranium(VI) cations.[30] The spectra of the two compounds showed a significant shift of the LMCT bands in the visible region. Spectral deconvolution allowed for assignment of the peak maxima; a red-shift of 0.32 eV was observed upon cation coordination. The lower energy charge transfer band observed in **4-tol** suggests that the charge transfer occurs to a lower energy unfilled orbital centered on the uranium cation. From these data we may infer that the potassium ions are bound to the uranyl oxo ligands in solution, and that coordination of the potassium ions lowers the energy of unfilled 5f-orbitals on uranium, the putative acceptor orbitals of the charge transfer transitions. To further support this assignment, we performed excited state calculations on **4-tol** and **4-crown**.
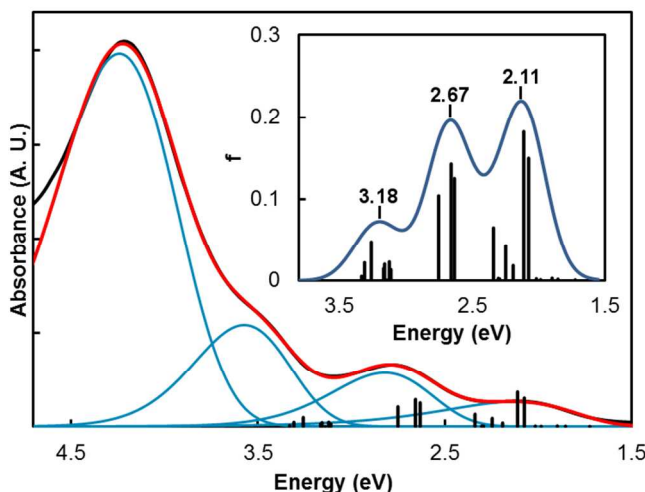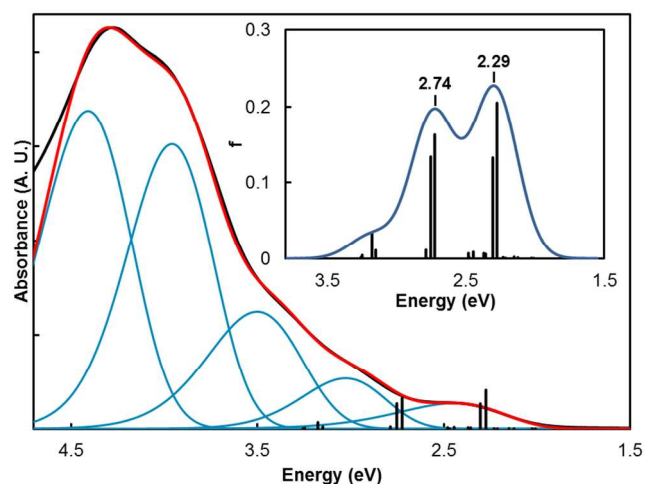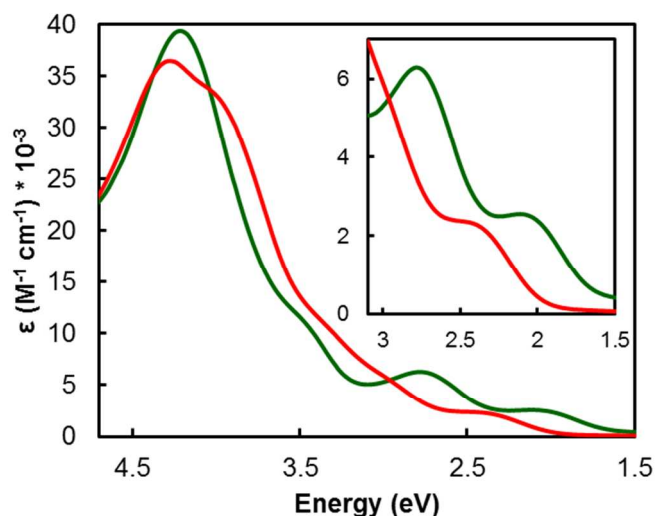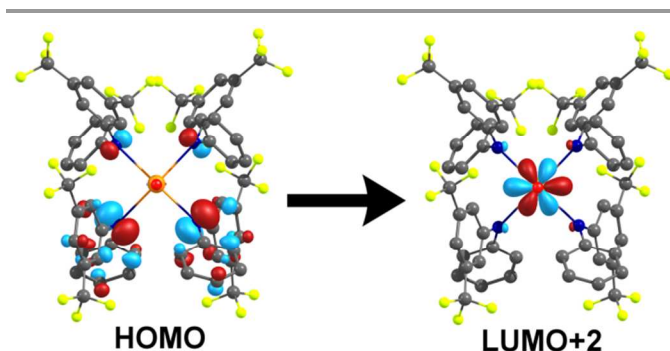

Fig. 7 Electronic absorption spectra of **4-tol** (green) and **4-crown** (red) in CH$_2$Cl$_2$.

Fig. 8 Spectral deconvolution of electronic absorption spectra of **4-crown** (top) and **4-tol** (bottom). Experimental data are shown in black, component peaks are shown in blue, and the fits is shown in red. Vertical black lines indicate TD-DFT calculated excitations, with simulated spectra inset.

Table 2 Crystallographic details.

	1	2	3	4-tol	4-crown
Chemical Formula	$C_{60}H_{48}F_{30}KN_3O_8U$	$C_{94}H_{114}F_{20}K_2N_4O_{12}U$	$C_{49}H_{44}F_{15}KN_6O_6U$	$C_{70}H_{48}F_{24}K_2N_4O_2U$	$C_{88}H_{100}F_{24}K_2N_4O_{18}U$
Formula Mass	1786.14	2188.12	1375.03	1749.35	2273.95
Crystal System	monoclinic	monoclinic	orthorhombic	monoclinic	monoclinic
a (Å)	20.0305(11)	34.3892(16)	16.6414(17)	15.9136(9)	14.2737(4)
b (Å)	16.0601(8)	15.7020(7)	19.756(2)	21.3308(13)	22.2064(7)
c (Å)	20.8994(10)	21.1110(9)	34.283(3)	22.1833(12)	32.9180(10)
α (°)	90.00	90.00	90.00	90.00	90.00
β (°)	96.967(3)	121.564(2)	90.00	110.360(3)	95.921(2)
γ (°)	90.00	90.00	90.00	90.00	90.00
Volume $(Å^3)$	6673.5(6)	9713.0(8)	11271.1(19)	7059.7(7)	10378.3(5)
Temperature (K)	143(1)	143(1)	143(1)	143(1)	143(1)
Space Group	$P2_1/c$	$C2/c$	$P2_12_12_1$	$P2_1/n$	$P2_1/c$
Z	4	4	8	4	4
Density (g/cm^3)	1.778	1.339	1.621	1.646	1.455
# Reflections Measured	199405	84416	186028	188472	157248
# Unique Reflections	15410	11131	25533	16272	23936
R_{int}	0.1622	0.0535	0.0416	0.0526	0.1032
R_1 [I > 2σ(I)]	0.0558	0.0566	0.0790	0.0309	0.0676
wR_2[I > 2σ(I)]	0.0982	0.1546	0.1973	0.0676	0.1636
R_1 (all data)	0.1525	0.1042	0.0900	0.0507	0.1237
wR_2 (all data)	0.1381	0.1736	0.2029	0.0750	0.1822

Fig. 9 Representative LMCT natural transition orbitals obtained from TD-DFT calculations, giving rise to the lowest energy absorption band in **4-tol** and **4-crown**.

TD-DFT calculations were performed on **4-tol** and the anionic portion of **4-crown**. The lowest energy transitions of significant oscillator strength were centered at 2.29 eV in **4-tol** and 2.11 eV in **4-crown**, in reasonably close agreement with the lowest energy bands in the experimental spectra at 2.43 eV in **4-tol** and 2.09 eV in **4-crown** (Fig. 8). These transitions were characterized as ligand to metal charge transfer (LMCT), primarily originating from nitrogen-centered non-bonding p-orbitals, excited into non-bonding uranium 5f orbitals. A representative transition is shown in Fig. 9, from the ligand-based HOMO to the metal-based LUMO+2. While the difference in energy of the charge transfer band in these two complexes is underestimated relative to the experimental results, the predicted red shift upon cation coordination and confirmation of these transitions as equatorial LMCT support the persistence of cation coordination in solution and the activation of the uranyl moiety by the K$^+$ ions. Consideration of

the ground state electronic structures of **4-tol** and **4-crown** yielded further insight into the extent of the activation. Direct K$^+$ coordination resulted in a lowering in energy of the U=O anti-bonding orbitals and a slight increase in the energy of the U–N anti-bonding orbitals, indicating destabilization of the axial U=O bonding and stabilization of the equatorial U–N bonding (Fig. 10).
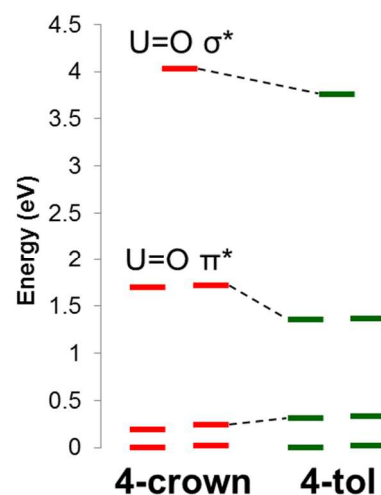
Fig. 10 Calculated unoccupied molecular orbitals of primarily uranium 5f character for **4-crown** and **4-tol**. Energies are shown relative to the LUMO for each complex. Orbitals depicted: (**4-crown**) LUMO–LUMO+3, LUMO+11, LUMO+12, LUMO+24; (**4-tol**) LUMO–LUMO+5, LUMO+34.

Finally, the impact of potassium ion coordination on the electronics of the uranyl ions in **4-tol** and **4-crown** was further assessed through electrochemical measurements. Notably, cyclic voltammetry performed in CH$_2$Cl$_2$ for both complexes

displayed different behavior between them (Fig. S2). Multiple quasi-reversible reduction processes were noted in **4-tol** at −1.6 and −1.9 V whereas a single highly irreversible process at a more negative potential of −2.3 V was observed for **4-crown**. The larger negative potential necessary to observe the first reduction feature in **4-crown** implies that the coordination of K^+ ion directly to the uranyl facilitates reduction. Lewis acid coordination to iron–oxo and manganese–oxo complexes is known to have a similar effect on metal complex reduction potentials.[51-55] The electrochemical data therefore further support the coordination of K^+ ion to **4-tol** in solution.

Conclusions

In the present work we have demonstrated the role of non-covalent cation-π and cation-F interactions in directing weak Lewis acid coordination to the weakly Lewis basic uranyl ion. The $NAr^FPh^−$ ligand was found to be best suited for directing K+ coordination. Experimental and computational data support the close association of K^+ ions in **4-tol** in solution. Collective, subtle interactions in the secondary coordination sphere therefore directly impact the electronic structure of the metal center. Incorporating supramolecular and self-assembly design principles into small molecular scaffolds continues to hold promise as a method to manipulate the coordination chemistry and reactivity of uranium. Further experiments using diverse Lewis acids and their effects on the vibrational spectroscopic characteristics of the uranyl cation, as well as experiments toward chemical functionalization of uranyl, are currently underway.

Acknowledgements

Notes and references

[a] Department of Chemistry, University of Pennsylvania, 231 S. 34th Street, Philadelphia, PA, USA.

Electronic Supplementary Information (ESI) available: Synthetic details and characterization, electrochemical data, IR data, details of X-ray crystallography experiments and computational details. See DOI: 10.1039/b000000x/ CCDC numbers: 965029-965033.

1. R. G. Denning, *J. Phys. Chem. A*, 2007, **111**, 4125.
2. L. Newsome, K. Morris and J. R. Lloyd, *Chem. Geol.*, 2014, **363**, 164.
3. S. Fortier and T. W. Hayton, *Coord. Chem. Rev.*, 2010, **254**, 197.
4. S. Kannan, M. A. Moody, C. L. Barnes and P. B. Duval, *Inorg. Chem.*, 2006, **45**, 9206.
5. E. O'Grady and N. Kaltsoyannis, *J. Chem. Soc., Dalton Trans.*, 2002, 1233.
6. B. Kosog, H. S. La Pierre, F. W. Heinemann, S. T. Liddle and K. Meyer, *J. Am. Chem. Soc.*, 2012, **134**, 5284.
7. H. S. La Pierre and K. Meyer, *Inorg. Chem.*, 2013, **52**, 529.
8. A. J. Lewis, P. J. Carroll and E. J. Schelter, *J. Am. Chem. Soc.*, 2013, **135**, 511.
9. A. J. Lewis, P. J. Carroll and E. J. Schelter, *J. Am. Chem. Soc.*, 2013, **135**, 13185.
10. M. J. Sarsfield and M. Helliwell, *J. Am. Chem. Soc.*, 2004, **126**, 1036.
11. P. L. Arnold, G. M. Jones, S. O. Odoh, G. Schreckenbach, N. Magnani and J. B. Love, *Nat. Chem.*, 2012, **4**, 221.
12. P. L. Arnold, D. Patel, C. Wilson and J. B. Love, *Nature*, 2008, **451**, 315.
13. D. D. Schnaars, G. Wu and T. W. Hayton, *J. Am. Chem. Soc.*, 2009, **131**, 17532.
14. D. D. Schnaars, G. Wu and T. W. Hayton, *Inorg. Chem.*, 2011, **50**, 4695.
15. D. D. Schnaars, G. Wu and T. W. Hayton, *Inorg. Chem.*, 2011, **50**, 9642.
16. J. L. Brown, C. C. Mokhtarzadeh, J. M. Lever, G. Wu and T. W. Hayton, *Inorg. Chem.*, 2011, **50**, 5105.
17. J. L. Brown, G. Wu and T. W. Hayton, *J. Am. Chem. Soc.*, 2010, **132**, 7248.
18. P. L. Arnold, A.-F. Pécharman and J. B. Love, *Angew. Chem. Int. Ed.*, 2011, **50**, 9456.
19. P. L. Arnold, E. Hollis, F. J. White, N. Magnani, R. Caciuffo and J. B. Love, *Angew. Chem. Int. Ed.*, 2011, **50**, 887.
20. P. L. Arnold, A.-F. Pécharman, E. Hollis, A. Yahia, L. Maron, S. Parsons and J. B. Love, *Nat. Chem.*, 2010, **2**, 1056.
21. P. L. Arnold, E. Hollis, G. S. Nichol, J. B. Love, J.-C. Griveau, R. Caciuffo, N. Magnani, L. Maron, L. Castro, A. Yahia, S. O. Odoh and G. Schreckenbach, *J. Am. Chem. Soc.*, 2013, **135**, 3841.
22. G. M. Jones, P. L. Arnold and J. B. Love, *Chem. - Eur. J.*, 2013, **19**, 10287.
23. G. M. Jones, P. L. Arnold and J. B. Love, *Angew. Chem. Int. Ed.*, 2012, **51**, 12584.
24. P. L. Arnold, G. M. Jones, Q.-J. Pan, G. Schreckenbach and J. B. Love, *Dalton Trans.*, 2012, **41**, 6595.
25. P. L. Arnold, D. Patel, A. J. Blake, C. Wilson and J. B. Love, *J. Am. Chem. Soc.*, 2006, **128**, 9610.
26. T. S. Franczyk, K. R. Czerwinski and K. N. Raymond, *J. Am. Chem. Soc.*, 1992, **114**, 8138.
27. J. A. Danis, M. R. Lin, B. L. Scott, B. W. Eichhorn and W. H. Runde, *Inorg. Chem.*, 2001, **40**, 3389.
28. B. Masci and P. Thuery, *CrystEngComm*, 2007, **9**, 582.
29. P. Thuéry, B. Masci, M. Takimoto and T. Yamato, *Inorg. Chem. Commun.*, 2007, **10**, 795.
30. M. J. Sarsfield, M. Helliwell and J. Raftery, *Inorg. Chem.*, 2004, **43**, 3170.
31. C. J. Burns, D. L. Clark, R. J. Donohoe, P. B. Duval, B. L. Scott and C. D. Tait, *Inorg. Chem.*, 2000, **39**, 5464.
32. L. A. Seaman, D. D. Schnaars, G. Wu and T. W. Hayton, *Dalton Trans.*, 2010, **39**, 6635.
33. P. Thuery and B. Masci, *Dalton Trans.*, 2003, 2411.
34. L. A. Seaman, P. Hrobarik, M. F. Schettini, S. Fortier, M. Kaupp and T. W. Hayton, *Angew. Chem. Int. Ed.*, 2013, **52**, 3259.
35. H. Yin, A. J. Lewis, U. J. Williams, P. J. Carroll and E. J. Schelter, *Chem. Sci.*, 2013, **4**, 798.

Dalton Transactions Accepted Manuscript

36. A. J. Lewis, U. J. Williams, J. M. Kikkawa, P. J. Carroll and E. J. Schelter, *Inorg. Chem.*, 2012, **51**, 37.

37. J. R. Robinson, P. J. Carroll, P. J. Walsh and E. J. Schelter, *Angew. Chem., Int. Ed. Engl.*, 2012, **51**, 10159.

38. J. R. Levin, J. Gu, P. J. Carroll and E. J. Schelter, *Dalton Trans.*, 2012, **41**, 7870.

39. H. Yin, A. J. Lewis, P. Carroll and E. J. Schelter, *Inorg. Chem.*, 2013, **52**, 8234.

40. H. Yin, A. J. Lewis, P. Carroll and E. J. Schelter, *Inorg. Chem.*, 2013.

41. H. Yin, J. R. Robinson, P. J. Carroll, P. J. Walsh and E. J. Schelter, *Chem. Commun.*, 2014, **50**, 3470.

42. D. R. Click, B. L. Scott and J. G. Watkin, *Chem. Commun.*, 1999, 633.

43. F. Allen, *Acta Crystallogr., Sect. B: Struct. Sci*, 2002, **58**, 380.

44. J.-C. Berthet, G. Siffredi, P. Thuery and M. Ephritikhine, *Chem. Commun.*, 2006, **0**, 3184.

45. L. Natrajan, F. Burdet, J. Pécaut and M. Mazzanti, *J. Am. Chem. Soc.*, 2006, **128**, 7152.

46. Direct crystallization of this product from hexanes was attempted several times, which produced complexes of variable K-THF solvation in which the potassium ions were bound directly to the uranyl oxo ligands. The variable solvation of this product prevented adequate structural refinement or full characterization.

47. J.-C. Berthet, G. Siffredi, P. Thuery and M. Ephritikhine, *Dalton Trans.*, 2009, **0**, 3478.

48. S. Beer, O. B. Berryman, D. Ajami and J. Rebek Jr, *Chem. Sci.*, 2010, **1**, 43.

49. A. J. Lewis, U. J. Williams, P. J. Carroll and E. J. Schelter, *Inorg. Chem.*, 2013, **52**, 7326.

50. A. Marini, A. Muñoz-Losa, A. Biancardi and B. Mennucci, *J. Phys. Chem. B*, 2010, **114**, 17128.

51. Y. J. Park, J. W. Ziller and A. S. Borovik, *J. Am. Chem. Soc.*, 2011, **133**, 9258.

52. S. Fukuzumi, Y. Morimoto, H. Kotani, P. Naumov, Y.-M. Lee and W. Nam, *Nat. Chem.*, 2010, **2**, 756.

53. E. Y. Tsui, R. Tran, J. Yano and T. Agapie, *Nat. Chem.*, 2013, **5**, 293.

54. C. G. Miller, S. W. Gordon-Wylie, C. P. Horwitz, S. A. Strazisar, D. K. Peraino, G. R. Clark, S. T. Weintraub and T. J. Collins, *J. Am. Chem. Soc.*, 1998, **120**, 11540.

55. W. W. Y. Lam, S.-M. Yiu, J. M. N. Lee, S. K. Y. Yau, H.-K. Kwong, T.-C. Lau, D. Liu and Z. Lin, *J. Am. Chem. Soc.*, 2006, **128**, 2851.

Dalton Transactions Accepted Manuscript

Dalton Transactions

ARTICLE

(Graphical Absract)